EBioMedicine 56 (2020) 102797

Contents lists available at ScienceDirect

EBioMedicine

journal homepage: www.elsevier.com/locate/ebiom

Research paper

# Obesity induces preadipocyte CD36 expression promoting inflammation via the disruption of lysosomal calcium homeostasis and lysosome function

Xiaoxiao Luo[a,1], Yanping Li[a,1], Ping Yang[a], Yao Chen[d], Li Wei[a], Ting Yu[a], Jun Xia[a], Xiong Z. Ruan[a,b,c], Lei Zhao[a,*], Yaxi Chen[a,*]

[a] Centre for Lipid Research, Key Laboratory of Molecular Biology for Infectious Diseases, Ministry of Education, Department of Infectious Diseases, Institute for Viral Hepatitis, The Second Affiliated Hospital, Chongqing Medical University, Chongqing 400016, China
[b] National Clinical Research Center for Aging and Medicine, Huashan Hospital, Fudan University, Hanghai, China
[c] John Moorhead Research Laboratory, Centre for Nephrology, University College London Medical School, Royal Free Campus, University College London, London, United Kingdom
[d] Medical Examination Center, The Second Affiliated Hospital, Chongqing Medical University, Chongqing, China

ARTICLE INFO

*Article History:*
Received 22 February 2020
Revised 13 April 2020
Accepted 28 April 2020
Available online 6 June 2020

*Keywords:*
CD36
Preadipocytes
Inflammation
Lysosomal calcium
IP3R1

ABSTRACT

*Background:* Preadipocyte is closely related to obesity-induced inflammation. The impairment of autophagic flux by defective lysosomal function has been observed in adipose tissue from obese mice. While the fatty acid translocase CD36 is an important immuno-metabolic receptor, it remains unclear whether preadipocyte CD36 is involved in adipose tissue inflammation and whether CD36 regulates lysosomal function.
*Methods:* Using visceral adipose tissue from obese patients, a high-fat diet (HFD)-induced obese mice model, primary mouse preadipocytes and 3T3L1 cells we analyzed whether and how preadipocyte CD36 modulates lysosomal function and adipose tissue inflammation.
*Findings:* CD36 expression in preadipocytes is induced in obese patients and HFD-fed mice, accompanied with the disruption of lysosome function. CD36 knockout protects primary preadipocytes of HFD-fed mice from lysosomal impairment. In vitro, CD36 interacts with Fyn to phosphorylate and activate Inositol (1,4,5)-trisphosphate receptor 1 (IP3R1), causing excess calcium transport from endoplasmic reticulum (ER) to lysosome, which results in lysosomal impairment and inflammation. Moreover, IP3R inhibitor 2-aminoethoxydiphenyl borate (2APB) attenuates lysosomal impairment, inflammation and lipid accumulation in CD36-overexpressing preadipocytes.
*Interpretation:* Our data support that the abnormal upregulation of CD36 in preadipocytes may contribute to the development of adipose tissue inflammation. CD36/Fyn/IP3R1-mediated lysosomal calcium overload leads to lysosomal impairment and inflammation in preadipocyte. Thus targeting improving lysosomal calcium homeostasis may represent a novel strategy for treating obesity-induced inflammation.


## 1. Introduction

Obesity is defined as excessive fat accumulation, which is characterized by an increase in the volume and number of adipose cells in white adipose tissue [1]. In 2015, 107.7 million children and 603.7 million adults were obese [2].

Obesity is often accompanied by low-grade chronic inflammation, which plays a crucial role in the development of obesity-related diseases, including type 2 diabetes, hypertension and cardiovascular diseases [3]. Adipose tissue is the main source of inflammatory cytokines in obesity [4]. Numerous studies have demonstrated that mature adipocytes secret proinflammatory cytokines and promote macrophages recruitment in adipose tissues, contributing to adipose tissue inflammation [5,6]. Preadipocytes are important cellular components of the stromal vascular fraction (SVF) derived from adipose tissue. In addition to its well-known capacity to differentiation into mature adipocytes, preadipocytes share numerous phenotypic features with pro-inflammatory macrophages [7]. The numbers of preadipocytes is significantly increased in adipose tissues from patients with obesity [8]. In response to fatty acid exposure, undifferentiated preadipocytes secrete higher levels of inflammatory cytokines/

* Corresponding authors.
*E-mail addresses:* zhaolei@cqmu.edu.cn (L. Zhao), chenyaxi@cqmu.edu.cn (Y. Chen).
[1] These authors contributed equally to this work.

https://doi.org/10.1016/j.ebiom.2020.102797

**Research in context**

*Evidence before this study*

Adipose tissue inflammation is closely related to obesity and obesity-related diseases. It has been reported that the lysosome plays a key role in both the priming and assembly phases of the inflammasome. The impairment of autophagic flux by defective lysosomal function has been observed in adipose tissue from obese mice, suggesting that lysosome may be important in obesity-induced adipose tissue inflammation. The fatty acid translocase CD36 is a multifunctional immuno-metabolic receptor. CD36 knockout protects mice from insulin resistance and reduces sterile inflammation via inhibiting JNK/NF-$\kappa$B/NLRP3 inflammasome pathway in adipocytes and macrophages. Studies have shown that in addition to mature adipocytes, preadipocytes are an important contributor to proinflammatory cytokines secretion as well as macrophage recruitment in adipose tissue. Although CD36 protein is usually undetected in preadipocytes, upregulation of CD36 in preadipocytes has been observed in familial combined hyperlipidaemia patients or 3T3L1 preadipocytes treated with oxidized-LDL. However, it was unclear whether preadipocyte CD36 expression was altered in obese patients and HFD-fed mice. Prior to this study it was also not known whether CD36 was involved in the maintenance of lysosomal function as well as the underlying mechanisms.

*Added value of this study*

We provide first evidence supporting that CD36 expression in preadipocytes was induced in obese patients and HFD-fed mice, accompanied with lysosomal impairment. CD36 knockout protected lysosomal impairment in primary preadipocytes from HFD-fed mice. In vitro, we demonstrated that CD36 interacted with Fyn to phosphorylate and activate IP3R1, causing excess calcium transport from ER to lysosome, which resulted in lysosomal impairment and inflammation in 3T3L1 preadipocytes. Moreover, IP3R inhibitor 2APB attenuated lysosomal impairment, inflammation and lipid accumulation in CD36-overexpressing preadipocytes.

*Implications of all the available evidence*

Our study opens a novel, expanded view on the pathogenesis of adipose tissue inflammation, suggesting that CD36/Fyn/IP3R1-mediated lysosomal calcium overload and lysosomal impairment in preadipocytes may be a potential new mechanism for obesity-induced inflammation. We proposed that improving lysosomal calcium homeostasis in particular in preadipocytes, as exemplified by the use of 2APB (IP3R inhibitor), represents a novel strategy for treating adipose tissue inflammation and obesity-related diseases.

chemokines (eg. MCP-1, and IL-6) than mature adipocytes [9–11]. Thus, these data suggest that preadipocyte may play an important role in the pathogenesis of obesity-related adipose tissue inflammation.

The fatty acid translocase CD36 is a widely expressed membrane glycoprotein that is involved in many physiological and pathological processes [12]. Several studies have shown that CD36 plays an important role in adipose tissue inflammation. Compared to wild-type (WT) mice, CD36 deficient mice with high-fat diet (HFD) exhibits reduced adipose tissue inflammation, as evidenced by decreased pro-inflammatory cytokine levels in adipose tissue, less macrophage and T-cell accumulation in adipose tissue [13,14]. In response to CD36 ligands (eg. ox-LDL and $\beta$-amyloid), CD36 mediates the activation of NF-$\kappa$B and/or inflammasome pathway, boosting sterile inflammation in macrophages and adipocytes [15,16]. Although CD36 protein is normally undetected in preadipocytes, its expression is induced during the differentiation of preadipocytes into mature adipocytes. Deficiency of CD36 attenuates adipogenesis in vivo [17]. The upregulation of preadipocytes CD36 expression is also observed in familial combined hyperlipidaemia patients and 3T3L1 preadipocytes treated with oxidized-LDL [18]. However, it remains unclear whether preadipocyte CD36 is altered in obese patients or HFD-fed mice. Prior to this study, it was also not known whether preadipocyte CD36 was involved in obesity-induced inflammation.

Accumulating evidence has suggested that lysosomal impairment is critical in the development of adipose tissue inflammation. Weber et al. found that inflammasomes are selectively activated through lysosome-dependent pathways in macrophages [19]. Impaired lysosomal function, which causes reduced autophagic clearance and inflammasome activation in the early stage of obesity, has also been observed in adipose tissue of obese mice [20]. The lysosome itself is an important calcium ($Ca^{2+}$) reservoir (0.5–0.6 mM $Ca^{2+}$) [21]. Impaired lysosomal $Ca^{2+}$ homeostasis causes lysosomal impairment and lysosomal storage diseases [22].

Inositol (1,4,5)-trisphosphate receptor 1 (IP3R1) is an important intracellular $Ca^{2+}$ release channel that plays a critical role in the regulation of endoplasmic reticulum (ER) $Ca^{2+}$ release [23]. Recent studies demonstrated that although IP3R not locate at the contact sites between ER and lysosome, it controls the redistribution of $Ca^{2+}$ from the ER to lysosome [23]. Previous studies showed that Fyn phosphorylates IP3R1 at Tyr353 and that this phosphorylation event is required for IP3-mediated $Ca^{2+}$ release in both B and T lymphocytes [24]. The downregulation of Fyn, by glucocorticoid and a selective Fyn inhibitor, prevents IP3R1 phosphorylation at Tyr353 and attenuates IP3-mediated $Ca^{2+}$ release in WEHI 7.2 T cells [25]. We have previously demonstrated that CD36-bound Fyn phosphorylates LKB1 to hinder AMPK-mediated $\beta$-oxidation in hepatocytes [26]. Thus, we postulated that CD36 interacts with Fyn, promoting Tyr353 phosphorylation of IP3R1, activating IP3R1-mediated $Ca^{2+}$ transfer from ER to lysosome, which consequently causes lysosomal impairment and inflammation in preadipocytes.

In this study, we provide several lines of evidence (using 3T3L1 preadipocytes cell lines, primary preadipocytes from mice, HFD-fed mice, as well as obese patient data) suggesting that obesity induces CD36 expression and lysosomal impairment in preadipocytes. CD36 deficiency alleviated HFD-induced lysosomal dysfunction in preadipocytes. We further showed that IP3R inhibitor 2-aminoethoxydiphenyl borate (2APB) attenuated lysosomal impairment, inflammation and lipid accumulation in CD36-overexpressing preadipocytes. We propose that improving lysosomal $Ca^{2+}$ homeostasis in particular in preadipocytes, represents a novel strategy for treating adipose tissue inflammation and obesity-related diseases.

## 2. Materials and methods

### 2.1. Study subjects

We conducted a cross-sectional analysis of 28035 subjects (15,912 males and 12,123 females) who underwent health examinations at the Affiliated Hospital of Chongqing Medical University (CQMU) from 2014 to 2015. Human visceral adipose tissue samples (7 obese patients and 7 non-obese patients) were obtained from patients who underwent laparoscopic cholecystectomy in the Affiliated Hospital of CQMU. The study was approved by the Ethics Committees of CQMU, and all subjects provided written informed consent. C57BL/6J mice, WT and CD36 knckout (CD36KO) mice were provided by Maria Febbraio (University of Alberta). Six-week-old mice were fed a HFD or normal diet (ND) for 14 weeks. All mouse care and experimental procedures were approved by the Institutional Animal Care and Use Committee of CQMU, and the investigation conforms with the Guidelines for the Care and Use of Laboratory Animals published by the US National Institutes of Health (NIH Publication No. 85-23, revised 1996).

### 2.2. Isolation of primary preadipocytes

Visceral adipose tissue from the mice was digested with 2 mg/ml collagenase D (Sigma-Aldrich, COLLD-RO) and 2.4 u/ml dispase II (Sigma-Aldrich, D4693) for 20 min at 37°C. The digestion reaction was terminated with culture medium before filtration. After centrifugation at 1000 rpm for 10 min, the precipitate was incubated with Alexa Fluor® 488 anti-mouse CD146 (BD Biosciences Cat# 562229, RRID: AB_11153320) / Alexa Fluor® 647 anti-mouse CD34 (BD Biosciences Cat# 560233, RRID:AB_1645199) for 30 min at 37°C. $CD146^-/CD34^+$ cells were separated by a FACScan flow cytometer (Becton-Dickinson). Then these $CD146^-/CD34^+$ cells were divided into 3 aliquots, which were respectively incubated with PE-CD36 (BD Biosciences Cat# 562702, RRID:AB_2737732), Lysotracker (Thermo Fisher Scientific, L7528) or Lysosensor Green (Thermo Fisher Scientific, L7535) for 30 min at 37°C. Cells incubated without antibody or with fluorescence-labeled isotype antibody (BD Biosciences Cat# 562141, RRID:AB_10894582) were negative (Neg) control or isotype control. The fluorescence signals were detected by a FACScan flow cytometer.

### 2.3. Plasmid and lentivirus production

The mammalian expression plasmid PCI-CD36 encoding full-length wild-type human CD36 cDNA was kindly provided by Kenneth J. Linton (University of London). Lentiviral constructs, including GV341 empty vector (Negative Control, NC), GV341 containing wild-type CD36 (wtCD36 OE), and GV341 containing the AA-SS mutant (mtΔCD36 OE), were provided by Shanghai GeneChem Company.

### 2.4. Cell culture

3T3L1 preadipocytes (ATCC Cat# CL-173, RRID:CVCL_0123) were maintained in Dulbecco's modified Eagle's medium (DMEM) supplemented with 10% calf serum. The 3T3L1 preadipocyte lines were maintained in 10% calf serum supplemented with puromycin (Sangon, A610593).

### 2.5. Cell viability assay

3T3L1 cells were seeded in 96-well plates at a density of 5000 cells/well and incubated for 24 h. The cells were then subjected to free fatty acid (FFA, 0.4 mM palmitate (PA)+0.2 mM oleic acid (OA)) loading for 60 h. The OD values were measured at 450 nm after incubation with CCK-8 reagent (Beyotime, C0042) for 2 h at 37°C.

### 2.6. Histology and immunohistochemical staining

Paraffin-embedded visceral adipose tissue sections were routinely stained with hematoxylin and eosin (HE). Immunohistochemical staining with anti-mouse F4/80 (Abcam Cat# ab6640, RRID: AB_1140040) or anti-CD36 (Novus Cat# NB 400-144, RRID:AB_522498) was performed to visualize the macrophage infiltration or the expression and localization of CD36 in adipose tissue. All images were captured using a Zeiss microscope. Image analysis was performed with ImageJ software.

### 2.7. Immunofluorescence staining and confocal microscopy

Paraffin-embedded visceral adipose tissue sections were incubated with anti-CD36 (Novus Cat# NB400-144, RRID:AB_10003498) anti-mouse Pref1 (R&D Systems, AF8277) or anti-human Pref1 (R&D Systems, MAB1144-SP), and then incubated with FITC-conjugated anti-rabbit IgG (ZSGB-Bio Cat# ZF-0311, RRID:AB_2571576), TRITC-conjugated anti-goat IgG (ZSGB-Bio, Cat# ZF-0317) or TRITC-conjugated anti-mouse IgG (ZSGB-Bio Cat# ZF-0313, RRID:AB_2571577). Finally, the sections were stained with DAPI (Boster, ar1176), and images were captured using a Leica confocal microscope. Cells were incubated with Lysotracker (Thermo Fisher Scientific, L7528) and BODIPY 493/503 (Thermo Fisher Scientific, D3922) or incubated with Lysotracker and Oregon Green™488 BAPTA-5N (Thermo Fisher Scientific, O6812). Then, images were captured using a Leica confocal microscope.

### 2.8. Lipid droplet staining

Cells were stained with 400 $\mu$M BODIPY 493/503 for 30 min and were captured by a Zeiss microscope. Cells were stained with 0.5% oil red O (Sangon, E607319) for 30 min, stained with hematoxylin for 5 min and then visualized with a Zeiss microscope.

### 2.9. Western blotting and co-immunoprecipitation

Equal amounts of protein were resolved and immunoblotted with anti-CD36 (Novus Cat# NB400-144, RRID:AB_10003498), anti-actin (Proteintech Cat# 20536-1-AP, RRID:AB_10700003), anti-NF-$\kappa$B p65 (Santa Cruz Biotechnology Cat# sc-8008, RRID:AB_628017), anti-Caspase-1 (Proteintech, 22915-1-AP), anti-IL-1$\beta$ (Proteintech Cat# 16806-1-AP, RRID:AB_10646432), anti-LaminB1 (Proteintech Cat# 12987-1-AP, RRID:AB_2136290), anti-P62 (Abcam Cat# ab109012, RRID: AB_2810880), anti-IP3R1 (GeneTex, GTX133104), anti-phospho-IP3R1 (Thermo Fisher Scientific Cat# PA5-64735, RRID:AB_2662549), and anti-Fyn (Proteintech, 66606-1-lg) primary antibodies. For co-immunoprecipitation (co-IP), equal amounts of lysate proteins were incubated (4°C) with anti-mouse CD36 (Novus Cat# NB600-1423, RRID: AB_789115) overnight before protein G magnetic beads were added (Millipore) (1−3 h). Bound proteins were eluted by boiling for 5 min in SDS sample buffer, and the cleared supernatants were resolved by SDS-PAGE. Detection was performed with the Chemidoc Imaging System (Bio-Rad) and ECL Plus reagent (Amersham). The band intensity was analyzed by densitometry software (ImageJ).

### 2.10. Autophagic flux analysis

Cells were first seeded in a confocal dish. After 24 h, cells were then transduced with mRFP-GFP-LC3 adenoviral vectors, which were purchased from HanBio Technology (Shanghai, China) according to the manufacturer's instructions. The principle of the assay is based on different pH stability of red and green fluorescent proteins. The EGFP fluorescent signal could be quenched under the acidic condition (pH below 5) inside the lysosome, whereas the mRFP fluorescent signal did not change significantly in acidic conditions. In red and green-merged images, autophagosomes are shown as yellow puncta, while autolysosomes are shown as red puncta.

### 2.11. Real-time RT-PCR

Total RNA was reversibly transcribed using PrimeScript RT reagent kit (DRR037A, TaKaRa, Biotech, Japan). Prepared cDNA was amplified using the LightCycler 96 system () and analyzed using SYBR Green PCR Master Mix (TaKaRa, Biotech, Japan). The cycle threshold (Ct) values were normalized to the amplification of mouse 36B4, and the data were analyzed using the ΔCt method. The primer sequences used in this study are shown in Supplementary Table 1. All primers were purchased from Beijing Genomics institution.

### 2.12. Transwell assay

THP-1 cells were purchased from Chinese Academy of Sciences Typical Culture Preservation Committee Cell Bank. THP-1 cells were added to the upper chambers. After phorbol 12-myristate 13-acetate (PMA)-induced THP-1 macrophage differentiation for 48 h, the culture supernatant of 3T3L1 preadipocytes was added to the lower chambers as a chemotactic factor. After incubation for 24 h, the migrated cells on the lower side of the membrane were fixed with

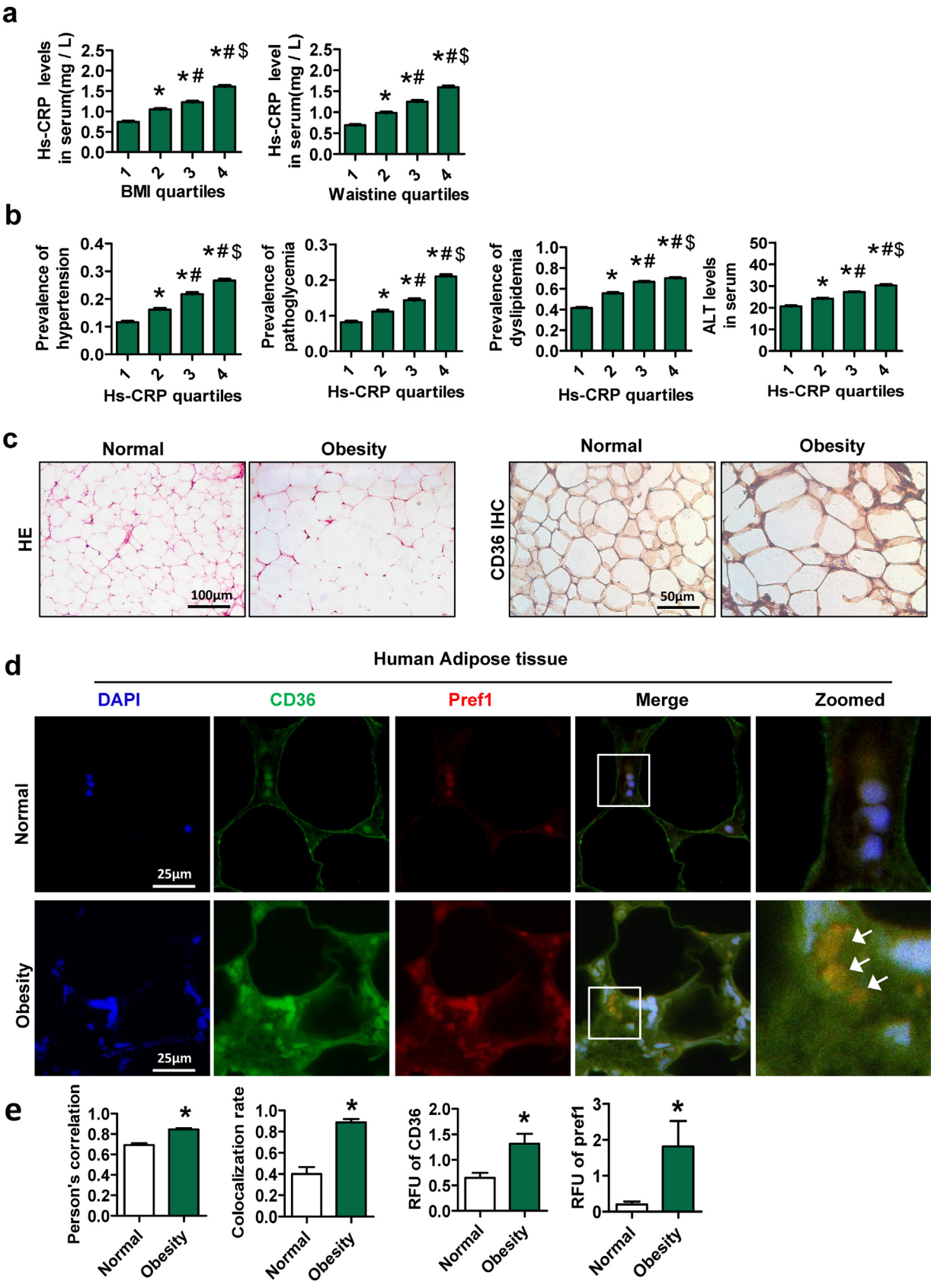


**Fig. 1.** Expression of CD36 in preadipocytes is induced in adipose tissue of obese patients. General health survey data were collected from 28,035 patients who underwent health examinations at the Affiliated Hospital of CQMU. Body mass index (BMI), waistline and serum hs-CRP measurements were divided into quartiles. The ranges of the different quartiles of BMI were <21.55 kg/m$^2$ (1st quartile), 21.55−23.66 kg/m$^2$ (2nd quartile), 23.66-25.81 kg/m$^2$ (3rd quartile) and >25.81 kg/m$^2$ (4th quartile). The ranges of the different quartiles of waist circumference were <76 cm (1st quartile), 76−82 cm (2nd quartile), 82−88 cm (3rd quartile) and 88 cm (4th quartile). The ranges of the different quartiles of hs-CRP were 0-0.30 mg/L (1st quartile), 0.31−0.60 mg/L (2nd quartile), 0.61−1.25 mg/L (3rd quartile) and >1.25 mg/L (4th quartile). Human visceral adipose tissue samples were obtained from patients who underwent laparoscopic cholecystectomy. The subjects were subdivided into two groups: non-obese patients (18.5 kg/m$^2$ <BMI<23.9 kg/m$^2$, $n$ = 7) and obese

ethanol and stained with crystal violet. The number of migrated cells was counted in five random fields under a microscope.

### 2.13. Detection of intracellular $Ca^{2+}$ and $Ca^{2+}$ release from the endoplasmic reticulum

Cells were incubated for 30 min in the presence of 0.5 $\mu$M fluo-4 AM (Beyotime, S1060), a $Ca^{2+}$ indicator dye, then washed twice with Hanks' balanced saline solution and allowed to incubate for 20 min before detection. The fluorescence intensity of intracellular $Ca^{2+}$ was monitored with a microplate reader prior to and following exposure to 1 $\mu$M thapsigargin (Sigma-Aldrich, T9033).

### 2.14. Statistical analysis

Continuous variables are presented as the mean ± standard error of the mean (SEM). High-sensitivity C-reactive protein (hs-CRP) was divided into 4 categories according to the quartile. Differences between two groups were statistically analyzed by Student's t-test. Differences among three or more groups were statistically analyzed by analysis of variance (one-way ANOVA) with Tukey's multiple comparisons test. A two-tailed p value of $<0.05$ was considered statistically significant.

## 3. Results

### 3.1. Expression of CD36 in preadipocytes is induced in adipose tissue of obese patients

A total of 28,035 participants (15,912 men and 12,123 women) were ultimately included in the analyses. The demographic and clinical characteristics of the subjects are summarized in Supplementary Table 2. As shown in Fig. 1a, the level of high-sensitivity C-reactive protein (hs-CRP) was positively associated with the BMI and waistline. In addition, the prevalence of dyslipidemia, hyperglycemia and hypertension, and alanine transaminase (ALT) was also positively correlated with hs-CRP (Fig. 1b). These findings suggested a close relationship between inflammation and obesity, as well as obesity-related metabolic disorders.

Compared with non-obese subjects, obese patients exhibited hypertrophic adipocytes and hyperplasia of SVF in visceral adipose tissue (Fig. 1c). Interestingly, we observed that the expression of CD36 was significantly increased in the SVF of visceral adipose tissue of obese patients (Fig. 1c). Next, we found that the expression of CD36 and Pref-1 (a marker of preadipocytes and mesenchymal precursors cells) [27,28] was increased in adipose tissue of obese patients compared with those of non-obese subjects (Fig. 1d and e). Moreover, the Pearson's correlation and colocalization rates of CD36 and Pref-1 were higher in obese patients than in non-obese subjects (Fig. 1e). These findings indicated that CD36 expression is increased in Pref-1 positive cells in adipose tissue from obese patients.

### 3.2. Expression of CD36 in preadipocytes is induced in HFD-fed mice accompanied with lysosomal impairment

We next investigated the role of CD36 in preadipocytes in obese mice. Six-week-old C57BL/6J mice were fed a HFD or ND for 14 weeks. Immunofluorescence results showed that the relative fluorescence units (RFUs) of CD36 and Pref-1 were higher in the C57-HFD group than in the C57-ND group (Fig. 2a). The Pearson's correlation and colocalization rates of CD36 and Pref-1 in the WT-HFD group were also higher than those in the ND group, which is consistent with the results from our clinical samples.

Since Pref-1 is a non-specific marker of preadipocytes, we used CD146-/CD34+ to isolate preadipocytes from SVF of adipose tissue in mice with a FACScan flow cytometer [29]. Compared with that in the C57-ND group, the percentage of preadipocytes in the C57-HFD group was increased (Fig. 2b). Meanwhile, the percentage of $CD36^+$ preadipocytes was increased, but the percentages of $Lysotracker^+$ and $Lysensor^+$ preadipocytes were decreased (Fig. 2c-e). Thus, our data suggested that HFD induces CD36 expression in preadipocytes, accompanied with lysosomal impairments.

### 3.3. CD36KO protects lysosomal impairment in primary preadipocytes from HFD-fed mice

We fed WT and CD36KO mice a HFD for 14 weeks and found that the percentage of preadipocytes was visibly decreased in the CD36KO-HFD group compared with the WT-HFD group (Fig. 3a). Interestingly, the percentages of $Lysotracker^+$ and $Lysosensor^+$ preadipocytes were increased in the CD36KO-HFD group compared with the WT-HFD group (Fig. 3b and c). These data suggested a protective effect of CD36KO on lysosomal impairment in primary preadipocytes from HFD-fed mice.

After 14 weeks of a HFD, compared with WT-HFD group, the CD36KO-HFD group showed no significant difference in body weight and the ratio of adipose tissue weight to body weight (Fig. 3d and e). Additionally, compared to the WT-HFD group, the CD36KO-HFD group exhibited increased glucose tolerance and insulin sensitivity (Fig. 3f and g). The expression of proinflammatory cytokines, including TNF$\alpha$, IL-1$\beta$, IL-6 and MCP-1, was increased in adipose tissue of the WT-HFD group (Fig. 3h). However, CD36KO decreased the expression of inflammatory cytokines in HFD-fed mice. HE and immunohistochemistry showed that adipocytes were enlarged and the SVF was hyperplastic in adipose tissue of the WT-HFD group compared with those of the WT-ND group and that these changes were accompanied by increased expression of F4/80 (Fig. 3i). However, SVF size and F4/80 expression were observably decreased in the CD36KO-HFD group. These results proved that CD36KO attenuates adipose tissue inflammation and insulin resistance (IR) in HFD-fed mice.

### 3.4. FFA upregulates CD36 expression and induces lysosomal impairment, lipid accumulation and inflammation in 3T3L1 preadipocytes

Next, we used FFA (a mixture of PA and OA) to mimic HFD condition [30]. As shown in Fig. 4a, FFA (0.4 mM PA+0.2 mM OA) exhibited no obvious toxicity effect on 3T3L1 preadipocytes. We found that FFA time-dependently increased CD36 expression in 3T3L1 preadipocytes (Fig. 4b). CD36 expression on the surface of 3T3L1 cells was significantly increased after FFA treatment (Fig. 4c). Compared with those in 3T3L1 preadipocytes without FFA treatment, lysosomal impairment was induced in 3T3L1 preadipocytes with FFA treatment, as evidenced by decreased median fluorescence intensity (MFI) of lysotracker and lysosensor (Fig. 4d). Moreover, 3T3L1 preadipocytes treated with FFA for 60 h showed more lipid droplets than control preadipocytes (Fig. 4e). The mRNA expression levels of inflammatory

patients (BMI≥28 kg/m$^2$, $n = 7$). (a) The serum contents of hs-CRP according to the BMI or waistline quartiles. (b) Prevalence of hypertension (systolic blood pressure≥140 mmHg or diastolic blood pressure≥90 mmHg), abnormal blood glucose (fasting blood glucose≥6.1 mmol/L) and dyslipidemia (total triglycerides≥1.7 mmol/L or cholesterol≥5.7 mmol/L or high-density lipoprotein<1 mmol/L or low-density lipoprotein≥3.12 mmol/L) according to hs-CRP quartiles. $^*p < 0.05$, compared with the first quartile at the same time point; $^\#p < 0.05$, compared with the second quartile at the same time point; $\$p < 0.05$, compared with the third quartile at the same time point. (c) HE staining and CD36 immunohistochemical staining of human adipose tissue. (d) Double immunofluorescence staining for CD36 and Pref1 in sections of human adipose tissue. The arrow indicates the colocalization area. (e) RFUs of CD36 and Pref-1. Pearson's correlation and colocalization rate of CD36 and Pref1. The data are presented as the mean ± SEM. Differences between the two groups were statistically analyzed by Student's $t$ test. $^*p < 0.05$ compared with the non-obese group.

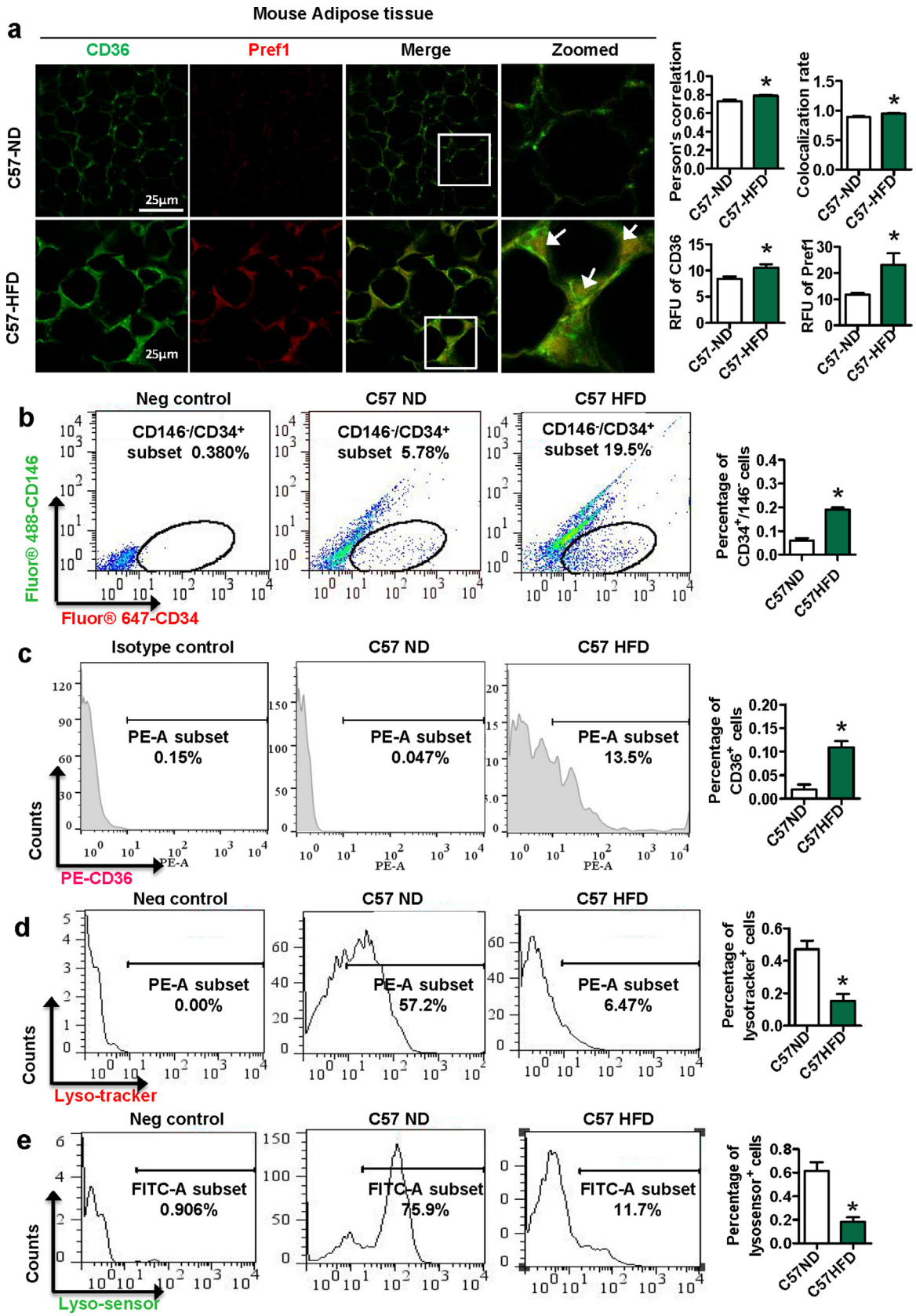


**Fig. 2.** Expression of CD36 in preadipocytes is induced in HFD-fed mice accompanied with lysosomal impairment. C57BL/6J mice were fed a HFD (5 males and 5 females) or normal diet (ND) (5 males and 5 females) for 14 weeks. (a) Double immunofluorescence staining for CD36 and Pref1 in sections of mouse adipose tissue. The arrow indicates the colocalization area. (b) Preadipocytes ($CD146^-/CD34^+$ cells) in mouse adipose tissue were sorted by a FACScan flow cytometer. CD36 expression (c) and lysosome function (d-e) in $CD146^-/CD34^+$ cells were detected by a FACScan flow cytomete. $^*p < 0.05$ compared with the C57-ND group.

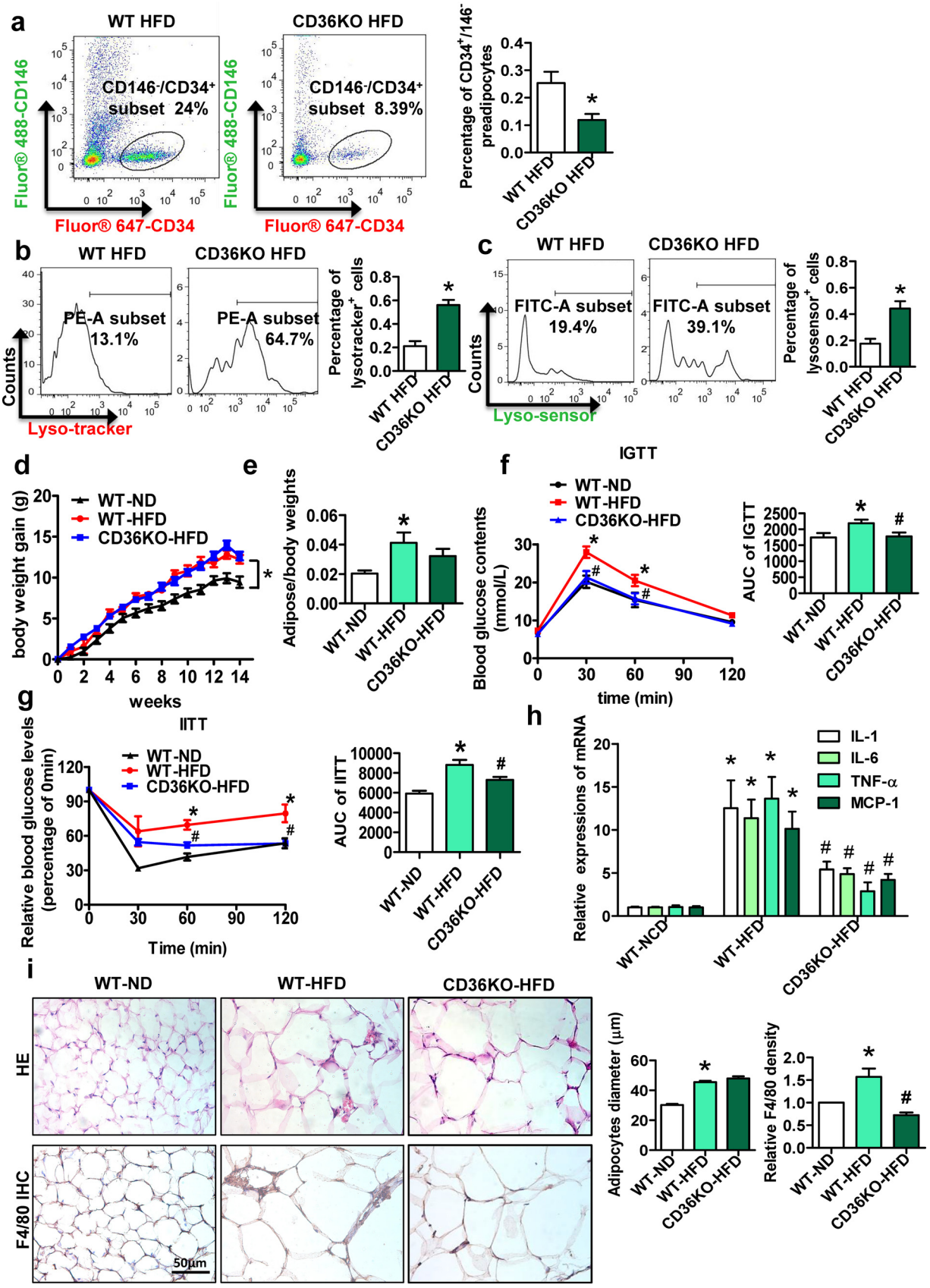


**Fig. 3.** CD36KO protects lysosomal impairment in primary preadipocytes from HFD-fed mice. WT mice were fed a HFD ($n = 6$) or ND ($n = 6$) for 14 weeks, and CD36KO mice were fed a HFD ($n = 6$) for 14 weeks. (a) Preadipocytes ($CD146^-/CD34^+$ cells) in mouse adipose tissue were sorted by a FACScan flow cytometer. (b and c) Lysosome function in $CD146^-/CD34^+$ cells were detected by a FACScan flow cytometer. The body weight (d) and the ratio of adipose tissue weight to body weight (e) of WT-ND, WT-HFD and CD36KO-HFD mice after feeding for 14 weeks. Intravenous glucose tolerance test results (f) and insulin tolerance test results intravenous (g) of WT-ND, WT-HFD and CD36KO-HFD mice after feeding for 14 weeks. (h) Relative mRNA expression of MCP1, TNF $\alpha$, IL-6 and IL-1$\beta$ in mouse adipose tissue. (i) Representative pictures of HE staining and F4/80 immunohistochemical staining in mouse adipose tissue. $^*p < 0.05$ compared with the WT-ND group. $\#p < 0.05$ compared with the WT-HFD group.

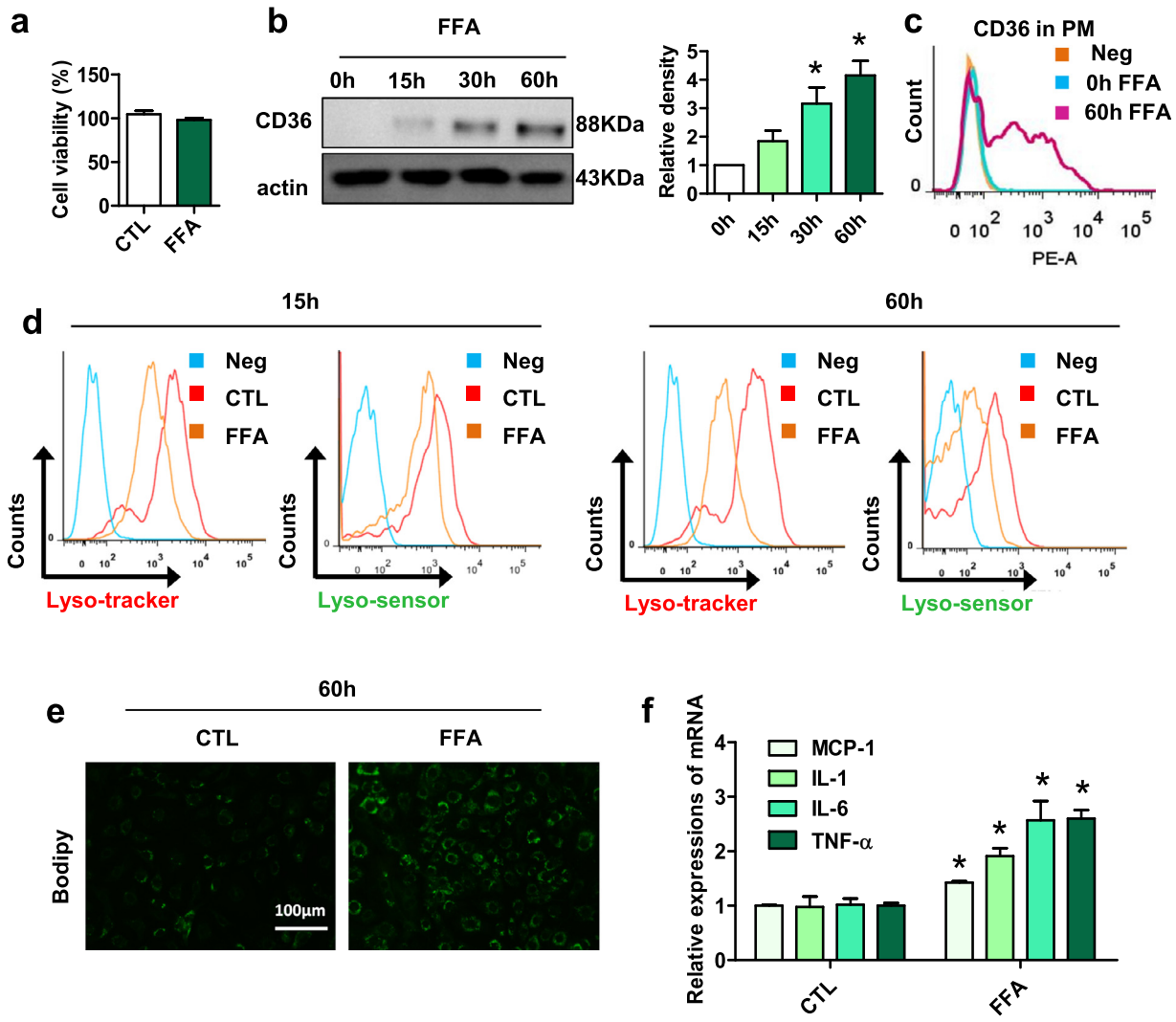


**Fig. 4.** FFA upregulates CD36 expression and induces lysosomal impairment, lipid accumulation and inflammation in 3T3L1 preadipocytes. (a) Cell viability assay in 3T3L1 preadipocytes treated with FFA for 60 h. (b) The relative protein expression of CD36 in 3T3L1 preadipocytes after treatment with FFA (0.4 mM PA+0.2 mM OA) for 15 h, 30 h and 60 h was detected by western blotting ($n$=3). $^*p$ <0.05 compared with 0h. (c) CD36 expression in plasma membrane (PM) of 3T3L1 preadipocytes treated with FFA for 0h and 60 h was detected by a FACScan flow cytometer ($n$=3). (d) Lysosome function in 3T3L1 preadipocytes treated with FFA for 15 h and 60 h were detected by a FACScan flow cytometer ($n$=3). (e) BODIPY staining of 3T3L1 preadipocytes treated with or without FFA (FFA group or control (CTL) group) for 60 h ($n$=3). (f) Relative mRNA levels of MCP1, TNF $\alpha$, IL-6 and IL-1$\beta$ in 3T3L1 preadipocytes treated with FFA for 60 h ($n$=3). $^*p$ <0.05 compared with the CTL group.

cytokines, including MCP-1, IL-1$\beta$, IL-6 and TNF$\alpha$, were also higher in 3T3L1 preadipocytes treated with FFA (Fig. 4f). These data indicated that FFA upregulates CD36 expression in 3T3L1 preadipocytes and that this upregulation is accompanied by lysosomal impairment, lipid accumulation and inflammation.

### 3.5. Forced CD36 upregulation induces lipid accumulation and inflammation in 3T3L1 preadipocytes

To further identify the role of CD36 in preadipocytes, we constructed wtCD36 OE preadipocyte lines and NC preadipocyte lines, respectively. Activated NF-$\kappa$B plays a key role in regulating inflammatory responses [31]. Compared with those in NC preadipocytes, the expression levels of NF-$\kappa$B p65, the ratio of caspase-1 p10 to pro-caspase-1 and the ratio of IL-1$\beta$ to pro-IL-1$\beta$ in wtCD36 OE preadipocytes were increased (Fig. 5a and b). Meanwhile, the mRNA expression levels of inflammatory cytokines, including MCP-1, IL-1$\beta$, IL-6 and TNF$\alpha$ were also higher in wtCD36 OE preadipocytes than in NC preadipocytes (Fig. 5c). These data demonstrated that CD36 overexpression upregulates inflammatory response in 3T3L1 preadipocytes by activating NF-$\kappa$B and the inflammasome.

Next, we cocultured THP-1 cells with preadipocytes and found that the number of migrated THP-1 cells was significantly increased in wtCD36 OE preadipocytes compared with NC preadipocytes (Fig. 5d), suggesting that wtCD36 OE in preadipocytes promoted cell migration. Then, Oil Red O and BODIPY staining showed that lipid accumulation was evident in wtCD36 OE preadipocytes compared with NC preadipocytes (Fig. 5e). These results further demonstrated that forced CD36 upregulation induces lipid accumulation and inflammation in 3T3L1 preadipocytes.

### 3.6. Forced CD36 upregulation impairs lysosomal function and lipophagy in 3T3L1 preadipocytes

As autophagy plays multiple roles in inflammatory responses and lipid accumulation, we then examined whether forced CD36 upregulation in 3T3L1 preadipocytes can regulate autophagy. We observed that the expression of P62 was increased in wtCD36 OE preadipocytes compared to NC preadipocytes (Fig. 6a). To further confirm the

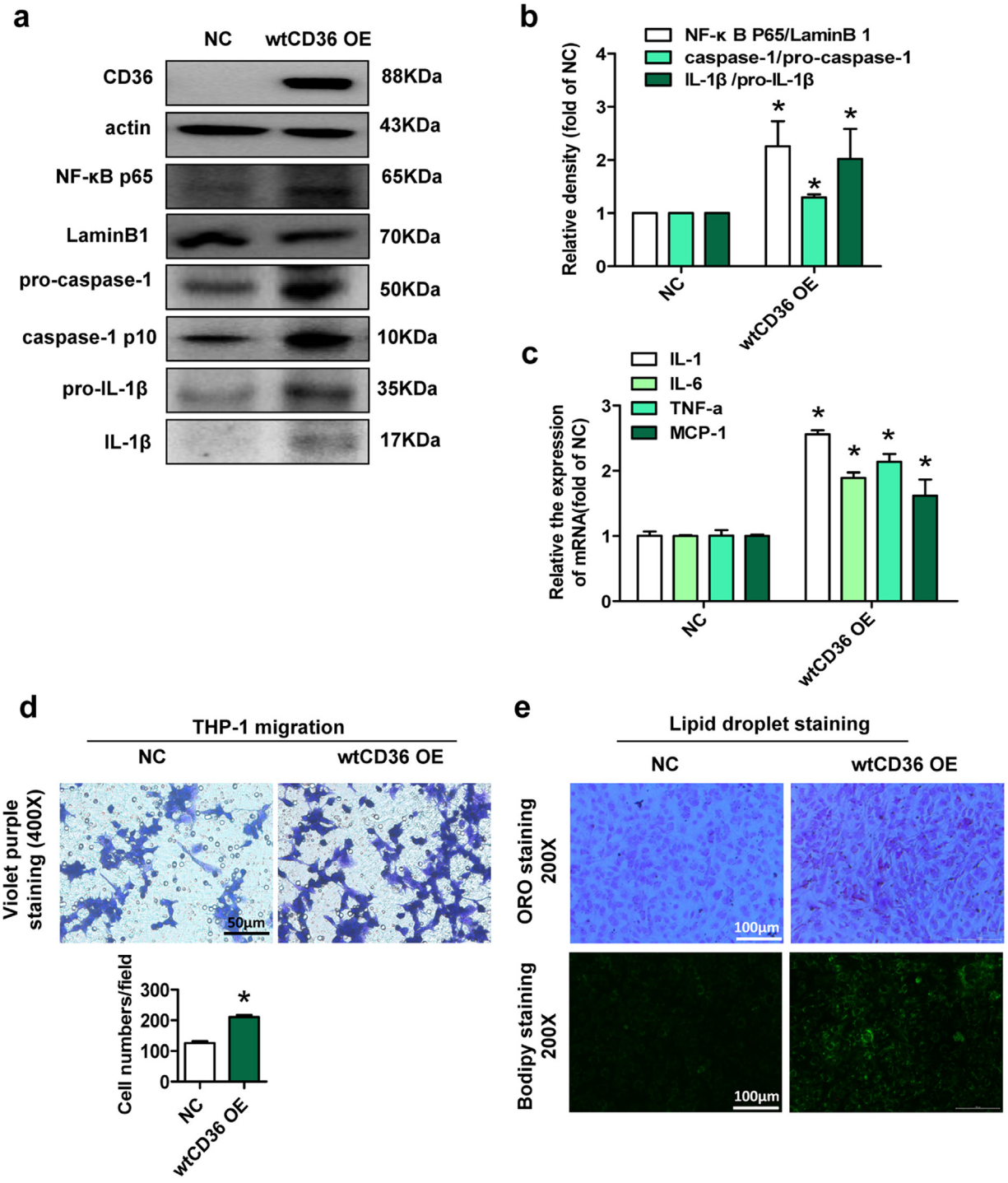


**Fig. 5.** Forced CD36 upregulation induces lipid accumulation and inflammation in 3T3L1 preadipocytes were infected with a recombinant lentivirus containing CD36 cDNA (wtCD36 OE preadipocytes) or empty vector (NC preadipocytes) and these cells were selected with puromycin. (a) Western blot analysis of CD36, NF-$\kappa$B p65, LaminB1, caspase-1, and IL-1$\beta$ in NC and wtCD36 OE preadipocytes ($n$=3). (b) The quantitative data of protein expression in A. (c) Relative mRNA levels of MCP1, TNF $\alpha$, IL-6 and IL-1$\beta$ in NC and wtCD36 OE preadipocytes ($n$=3). (d) Migration assay. A migration assay was performed by using Transwell migration chambers (8-$\mu$m pore size) to assess THP-1 cell migration co-cultured with the 3T3L1 preadipocyte lines ($n$=3). (e) BODIPY staining and oil red O staining of NC and wtCD36 OE preadipocytes ($n$=3). *$p$<0.05 compared with the NC group.

changes of autophagy flux, we transfected 3T3L1 preadipocytes with mRFP-GFP-LC3 adenoviral vectors. As shown in Fig. 6b, while the puncta-like LC3 protein was predominantly red in NC preadipocytes, those in wtCD36 OE preadipocytes tended to be yellow, suggesting either a lower capacity of lysosomes in the quenching of green fluorescence in lysosomes due to the elevated pH, or a block in the fusion of autophagosomes with lysosomes (Fig. 6b). Moreover, wtCD36 OE induced the lysosomal impairment, as evidenced by reduced MFI of lysotracker and lysosensor in wtCD36 OE preadipocytes (Fig. 6c). We further detected the location of lipids in lysosomes. There was weaker colocalization of lysotracker and BODIPY in wtCD36 OE preadipocytes than in NC preadipocytes (Fig. 6d). These findings showed

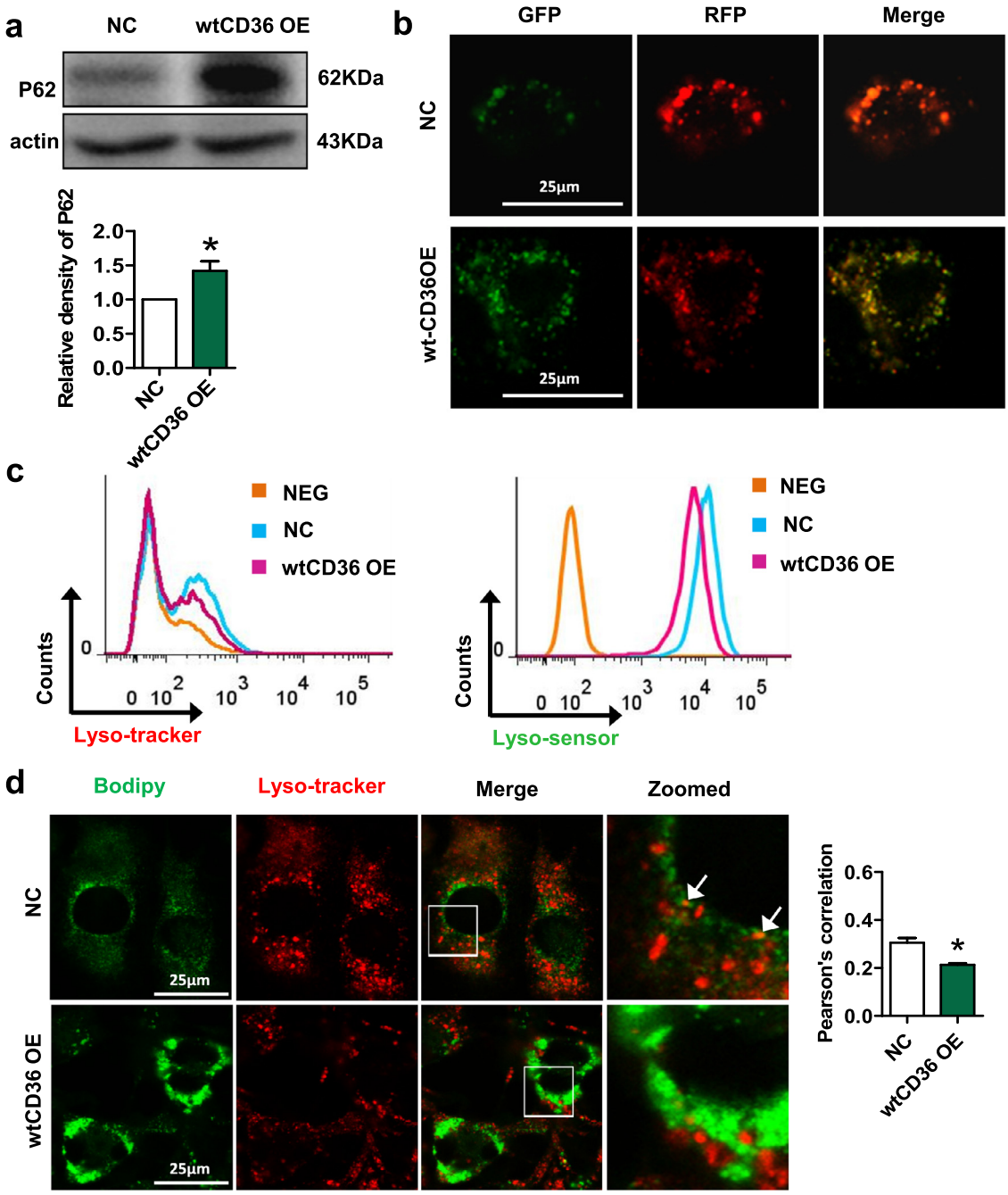


**Fig. 6.** Forced CD36 upregulation impairs lysosomal function and lipophagy in 3T3L1 preadipocytes. (a) Western blot analysis of P62 in NC and wtCD36 OE preadipocytes ($n$=3). (b) Double fluorescent staining of mRFP-GFP-LC3 fusion protein in NC and wtCD36 OE preadipocytes. (c) Lysosome function in NC and wtCD36 OE preadipocytes were detected by a FACScan flow cytometer ($n$=3). (d) Representative images showed double immunofluorescence staining for BODIPY and Lysotracker in wtCD36 OE and NC preadipocytes. The arrow indicates the colocalization area. $^{*}p<0.05$ compared with the NC group.

that forced CD36 upregulation impairs lysosomal function and lipophagy in 3T3L1 preadipocytes.

### 3.7. Forced CD36 upregulation promotes IP3R1-mediated $Ca^{2+}$ transport from the ER to lysosomes in preadipocytes

Since lysosomal $Ca^{2+}$ homeostasis plays an important role in the maintenance of lysosomal function [32], we next investigated the effect of CD36 on lysosomal $Ca^{2+}$ homeostasis in preadipocytes. Oregon Green® 488 BAPTA-5N (OG-BAPTA-5N) is a $Ca^{2+}$ indicator. We found that there was a higher Pearson's correlation coefficient of lysotracker and OG-BAPTA-5N in wtCD36 OE preadipocytes than in NC preadipocytes (Fig. 7a). IP3Rs are $Ca^{2+}$ release channels in the ER, and $Ca^{2+}$ released by IP3Rs can be rapidly, reversibly and selectively accumulated in lysosomes [33]. Three IP3R isoforms are expressed in mammals, but IP3R1 is the most extensively studied isoform. Notably, the activation and phosphorylation (at Tyr353) of IP3R1 were significantly increased in wtCD36 OE preadipocytes compared to NC preadipocytes (Fig. 7b). The IP3R antagonist 2-aminoethoxydiphenyl borate (2APB) attenuated the lysosomal impairment induced by wtCD36 OE, as well as the lipid accumulation and production of downstream mitochondrial reactive oxygen species (ROS) (Fig. 7c–f). Furthermore, 2APB suppressed the increased mRNA expression of inflammatory factors (MCP-1, IL-1, IL-6, and TNF-$\alpha$) induced by wtCD36 OE (Fig. 7g). These findings

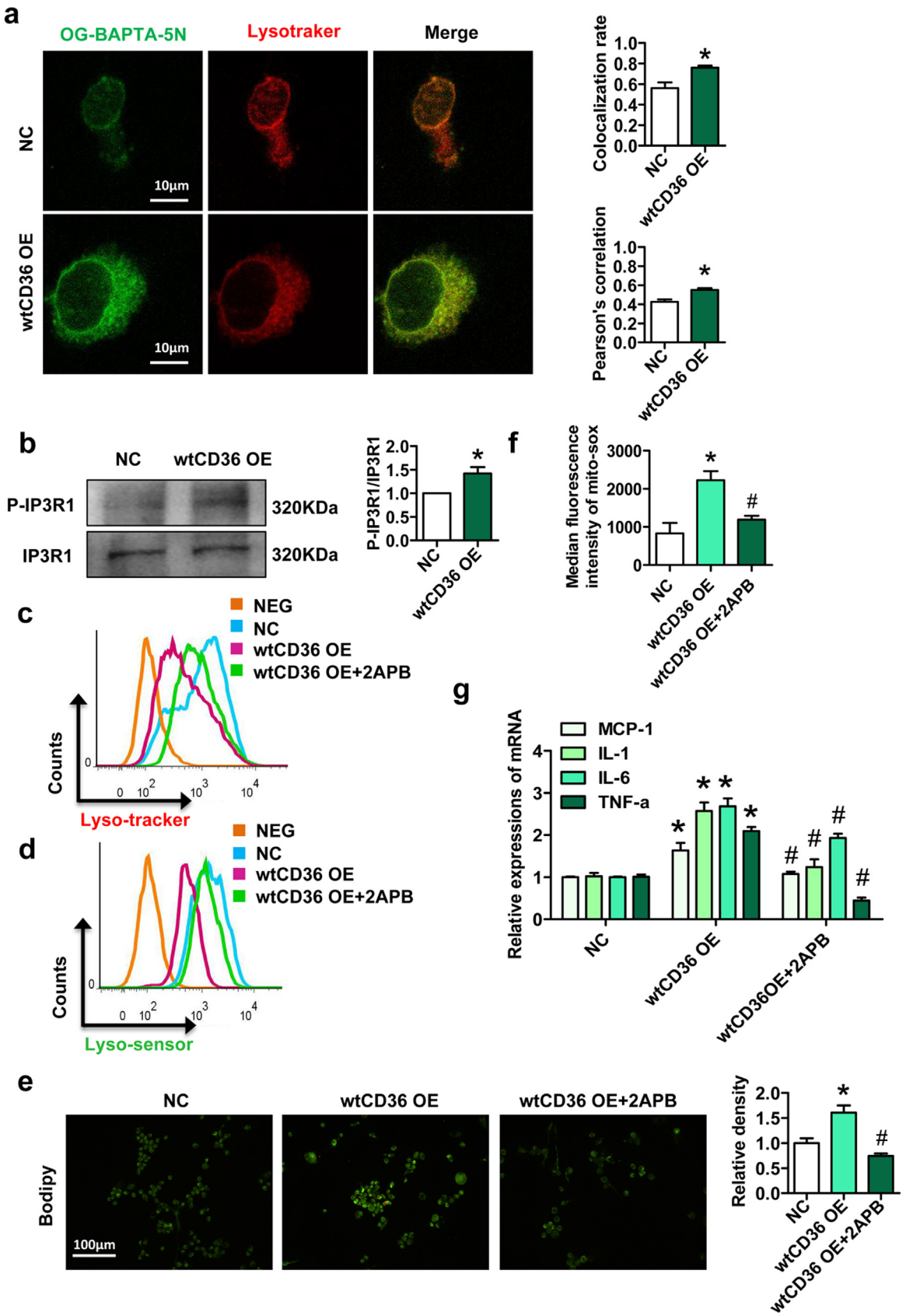


**Fig. 7.** Forced CD36 upregulation promotes IP3R1-mediated $Ca^{2+}$ transport from the ER to lysosomes in preadipocytes. (a) Representative images showed double immunofluorescence staining for OG-BAPTA-5N and lysotracker in wtCD36 OE and NC preadipocytes. (b) Western blot analysis of IP3R1 and P-IP3R1 (Tyr353) in wtCD36 OE preadipocytes and NC preadipocytes ($n$=3). After wtCD36 OE preadipocytes were treated with or without 2APB (0.5 $\mu$M) for 1 h, lysosome function (c-d) were detected by a FACScan flow cytometer ($n$=3). (e) BODIPY staining ($n$=3). (f) Mitochondrial reactive oxygen species assay ($n$=3). (g) Relative mRNA levels of MCP1, TNF $\alpha$, IL-6 and IL-1$\beta$. *$p$<0.05 compared with the NC group ($n$=3). #$p$<0.05 compared with the wtCD36 OE group.

presented evidence that forced CD36 upregulation promotes IP3R1 phosphorylation and activation, thus enhancing $Ca^{2+}$ transport from ER to lysosomes in preadipocytes.

### *3.8. CD36 coordinates with Fyn to phosphorylate IP3R1, inducing lysosomal $Ca^{2+}$ overload and inflammation in preadipocytes*

Since CD36 can interact with Fyn kinase of the Src family, we mutated the palmitoylation site of CD36 to weaken the binding of CD36 to Fyn [26]. Co-IP experiments demonstrated that the interaction between CD36 and Fyn was significantly reduced in mtΔCD36 OE preadipocytes compared with wtCD36 OE preadipocytes (Fig. 8a). Moreover, the expression of phosphorylated IP3R1 was decreased in mtΔCD36 OE preadipocytes compared with wtCD36OE preadipocytes, and this decrease in expression was accompanied by decreased cytoplasmic basal $Ca^{2+}$ levels, ER-released $Ca^{2+}$ levels, and lysosomal $Ca^{2+}$ levels (Fig. 8b–e). The Fyn inhibitor PP2 also inhibited the increase in lysosomal $Ca^{2+}$ levels induced by wtCD36 OE (Fig. 8e). Furthermore, the expression levels of NF-$\kappa$B and IL-1$\beta$ were significantly reduced in mtΔCD36 OE preadipocytes compared with wtCD36 OE preadipocytes (Fig. 8f). These data showed that CD36 coordinates with Fyn to phosphorylate IP3R1, inducing lysosomal $Ca^{2+}$ overload and inflammation in preadipocytes.

## 4. Discussion

Obesity has become a major global public health problem [34]. Previous studies have found that obesity markers, including BMI, waist circumference and percent body fat, are positively associated with hs-CRP. Yoon K et al. revealed that compared with lower hs-CRP level, relatively higher hs-CRP levels within the normal range may predict an increase in the occurrence of metabolic syndrome. Here, we also found that inflammation is associated with both the severity of obesity and the risk of adverse outcomes in obesity-associated diseases. Together with previous studies, our data demonstrated that inflammation is a common feature of obesity and links obesity to multiple metabolic diseases.

CD36 is a class B scavenger receptor involved in angiogenesis, atherosclerosis, and lipid metabolism [35]. In recent years, CD36 in adipocytes, macrophages and lymphocytes has been found to contribute to adipose tissue inflammation. CD36 deficiency reduces inflammatory phenotype and improves insulin signaling in primary adipocytes and macrophages isolated from HFD-fed mice [14]. Hematopoietic deletion of CD36 reduces macrophage recruitment and inflammatory profile of white adipose tissue [36]. In addition, CD36 expression in adipose T cells is increased in obese mice [37]. The accumulation of macrophages and T cells in adipose tissue was decreased in CD36 deficient mice with HFD [13]. In present study, we found that CD36 expression was upregulated in Pref-1 positive cells in adipose tissue of obese patients and HFD-fed mice, suggesting that CD36 expression was significantly induced in the SVF, but not in mature adipocytes. One possible explanation is that CD36 expression is already high in mature adipocytes. Then, we used CD146 and CD34 to characterize preadipocytes [29]. We found that the number of preadipocytes ($CD146^{-}/CD34^{+}$ cells) was increased in HFD-induced obese mice and that the number of preadipocytes was decreased in CD36KO mice with HFD. Furthermore, we used FFA to mimic the HFD condition and found that FFA induced CD36 expression in 3T3L1 preadipocytes in a time-dependent manner, which may at least partly, due to PA-induced increase of translational efficiency of CD36 protein, as we previously described [38]. Thus, we provide fine evidence supporting that preadipocytes CD36 is induced under obese conditions.

Our data also showed that HFD induced lysosomal impairment in primary preadipocytes. Both FFA treatment and the forced upregulation of CD36 caused lysosomal impairment and inflammation in 3T3L1 preadipocytes. Interestingly, CD36 deficiency protected HFD-induced lysosomal impairment in preadipocytes, accompanied with improved adipose tissue inflammation and IR in vivo. Thus, our data provide several lines of evidence that the pathological increase of CD36 in preadipocytes may contribute to the development of obesity-induced lysosomal impairment and inflammation. Interestingly, these events may not occur when CD36 is physiologically upregulated during the process of preadipocytes differentiation into adipocytes [39,40]. Moreover, due to the lack of preadipocyte-specific CD36KO mice, we do not observe the direct effects of preadipocytes CD36 in adipose tissue inflammation and obesity-related disorders in vivo. Further studies are required to achieve a fuller understanding of the role played by preadipocytes CD36 in the regulation of differentiation and adipose tissue inflammation.

The lysosome is a highly membrane-bound organelle that is important in protein degradation, cell signal transduction and inflammation [41]. Mounting evidence has demonstrated the lysosomal pathway as a key player in regulating the inflammatory response [42]. Lysosomal rupture triggers inflammasome activation in macrophages via the TAK1-JNK pathway [43]. Lysosomal destabilization also activates the inflammasome pathway, which promotes the production of IL-6 and IL-8 in an autocrine manner in human umbilical vein endothelial cells [44]. Moreover, the lysosome acts as an important intracellular $Ca^{2+}$ reservoir, and $Ca^{2+}$ homeostasis is important for the maintenance of lysosomal functions [33].

In this study, we found that the $Ca^{2+}$ level in lysosomes was significantly increased in wtCD36 OE preadipocytes compared with NC preadipocytes. Recent studies have suggested that lysosomes rapidly, reversibly and selectively accumulate $Ca^{2+}$ released by IP3Rs, key $Ca^{2+}$ release channels in the ER [45]. Antagonists of IP3Rs rapidly and completely block Ca2+ refilling of lysosomes, suggesting that IP3R-mediated ER release serves as a direct and primary source of $Ca^{2+}$ for the lysosome [46]. In mammals, there are three IP3R isoforms, namely, IP3R type 1 (IP3R1), IP3R type 2 (IP3R2), and IP3R type 3 (IP3R3), and IP3R1 is the most extensively studied isoform. Here, we also demonstrated that CD36 upregulation promoted the expression of phosphorylated IP3R1 and the release of $Ca^{2+}$ from the ER in preadipocytes. In addition, 2APB (an IP3R inhibitor) restored lysosomal function, reducing lipid accumulation and the inflammatory response in wtCD36 OE preadipocytes. These results suggested that CD36 activates IP3R1 to promote ER-lysosomal $Ca^{2+}$ transport, leading to lysosomal impairment. Moreover, our data supported that improving lysosomal Ca2+ homeostasis, such as the use of 2APB, is a compelling therapeutic approach in treating obesity-induced inflammation and obesity-related diseases.

The conductance of IP3R1 in the ER requires the activity of Src family kinases, such as Fyn. Although Fyn can probably phosphorylate more than one site on IP3R1, most of the phosphorylation occurs at a single site, i.e., Tyr353. In this study, we found that CD36 upregulation induced the phosphorylation (Tyr353) and activation of IP3R1 in preadipocytes. CD36 is crucial for Fyn activation and downstream signaling. The inhibition of CD36 palmitoylation decreases the CD36/Fyn complex in HepG2 cells [26]. Here, we mutated the palmitoylation site of CD36 to obtain a mutant (mtΔCD36 OE). The interaction of CD36 with Fyn was observably decreased in the mtΔCD36 group compared with the wtCD36 group. Interestingly, the phosphorylation and activation of IP3R1 (Tyr353) were significantly decreased in the mtΔCD36 group, resulting in reduced $Ca^{2+}$ release from the ER. Consequently, lysosomal $Ca^{2+}$ was reduced in the mtΔCD36 group and the wtCD36 group treated with PP2 (an inhibitor of Fyn). Moreover, the expression levels of inflammatory cytokines in the mtΔCD36 group were decreased compared with those in the respective controls.

In summary, our findings provide evidence supporting that the abnormal upregulation of CD36 in preadipocytes may contribute to the pathogenesis of obesity-induced lysosomal impairment and inflammation. CD36/Fyn/IP3R1-mediated lysosomal $Ca^{2+}$ overload in preadipocytes may be a potential new mechanism for obesity-related inflammation. Moreover, IP3R inhibitor 2APB attenuated lysosomal

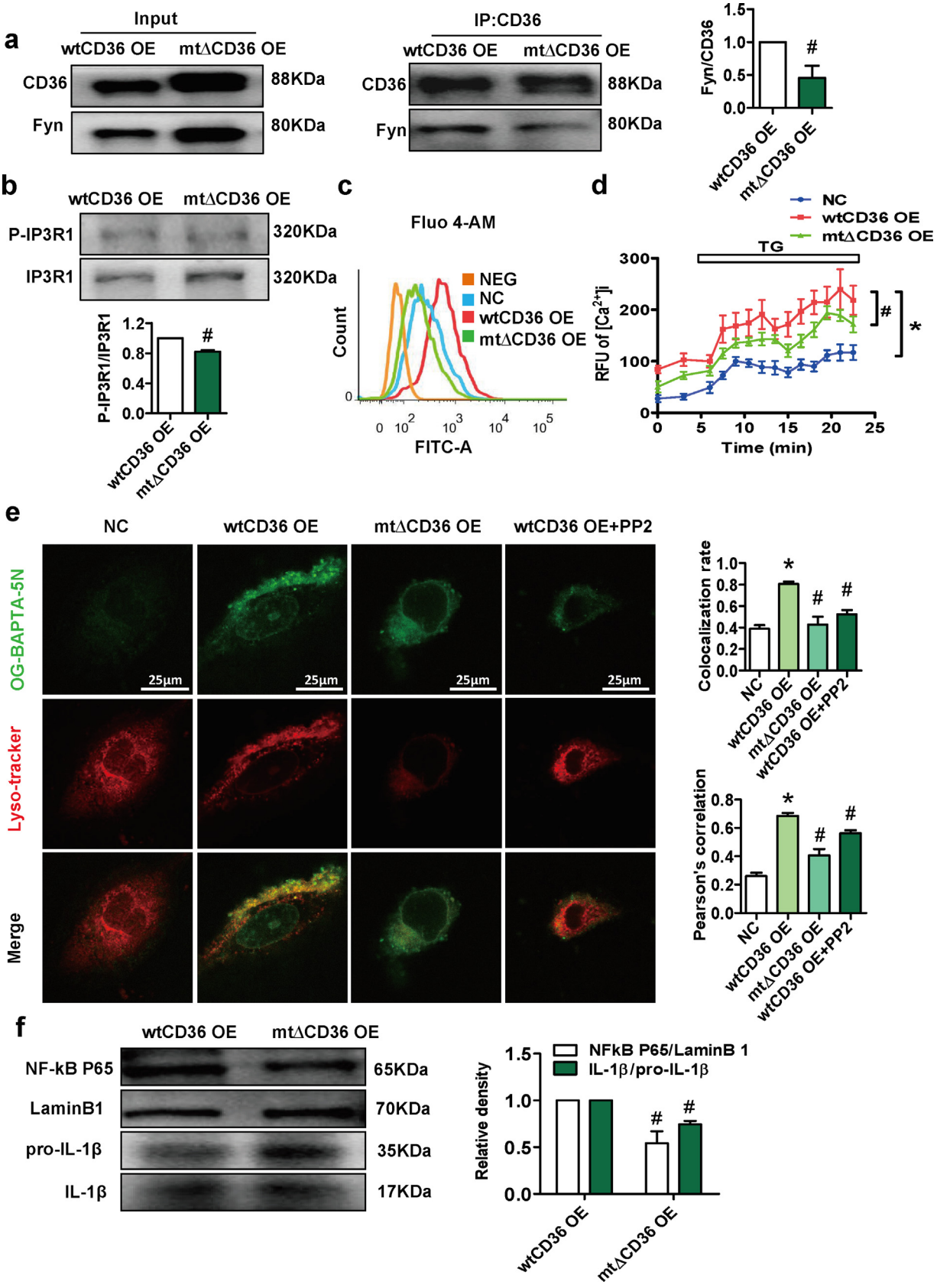


**Fig. 8.** CD36 coordinates with Fyn to phosphorylate IP3R1, inducing lysosomal $Ca^{2+}$ overload and inflammation in preadipocytes. We constructed a lentivirus containing CD36 with a palmitoylation site mutation and infected the 3T3L1 cells with lentivirus (mtΔCD36 OE preadipocytes). (a) Co-IP for CD36 and Fyn in wtCD36 OE preadipocytes and mtΔCD36 OE preadipocytes ($n$=3). (b) Western blot analysis of IP3R1 and P-IP3R1 (Tyr353) in wtCD36 OE preadipocytes and mtΔCD36 OE preadipocytes ($n$=3). (c) Cells were incubated for 30 min in the presence of 0.5 $\mu$M fluo-4 AM, a $Ca^{2+}$ indicator dye, to detect total intracellular $Ca^{2+}$ ($n$=3). (d) ER $Ca^{2+}$ release assay. Cells were incubated with fluo-4 AM (0.5 $\mu$M) for 30 min. Intracellular $Ca^{2+}$ was monitored prior to and following exposure to 1 $\mu$M thapsigargin ($n$=3). (e) Representative images showed double immunofluorescence staining for OG-BAPTA-5N and Lysotracker in NC preadipocytes, wtCD36 OE preadipocytes (treated with or without PP2) and mtΔCD36 OE preadipocytes. (f) Western blot analysis of NF-kB and IL-1$\beta$ in wtCD36 OE preadipocytes and mtΔCD36 OE preadipocytes ($n$=3). *$p$<0.05 compared with the NC group. #$p$<0.05 compared with the wtCD36 OE group.

impairment, inflammation and lipid accumulation in wtCD36 OE preadipocytes. Thus we proposed that improving lysosomal $Ca^{2+}$ homeostasis in particular in preadipocytes, as exemplified by the use of 2APB, represents a novel strategy for treating adipose tissue inflammation and obesity-related diseases.

## Declaration of Competing Interest

The authors declare that they have no conflict of interest.

## Funding sources

This work was supported by National Key R&D Program of China (2018YFC1312700), the National Natural Science Foundation of China (81873569, 81970510, 31971084) the Science and Technology Research Program of Chongqing Municipal Education Commission (KJZD-K201800401, KJQN201900438) and Talent Project of Chongqing (CQYC2019050790). The funders above did not have any involvement in the study design, data collection, data analysis, interpretation, and manuscript writing.

## Author contributions

XXL, YPL, TY and JX performed the experiments. PY, YC, LW and XZR analyzed the data. XXL, YPL, LZ prepared figures and contributed to the drafting of the manuscript. LZ, YXC designed the study, supervised this work and edited and revised manuscript. All authors critically reviewed the manuscript.

## Supplementary materials

Supplementary material associated with this article can be found in the online version at doi:10.1016/j.ebiom.2020.102797.

## References

[1] Prospective Studies C, Whitlock G, Lewington S, et al. Body-mass index and cause-specific mortality in 900 000 adults: collaborative analyses of 57 prospective studies. Lancet 2009;373(9669):1083–96.
[2] Collaborators GBDO, Afshin A, Forouzanfar MH, et al. Health Effects of Overweight and Obesity in 195 Countries over 25 Years. N Engl J Med 2017;377(1):13–27.
[3] Guo W, Wong S, Xie W, Lei T, Luo Z. Palmitate modulates intracellular signaling, induces endoplasmic reticulum stress, and causes apoptosis in mouse 3T3-L1 and rat primary preadipocytes. Am J Physiol Endocrinol Metab 2007;293(2):E576–86.
[4] Lumeng CN, Saltiel AR. Inflammatory links between obesity and metabolic disease. J Clin Invest 2011;121(6):2111–7.
[5] Kanda H, Tateya S, Tamori Y, et al. MCP-1 contributes to macrophage infiltration into adipose tissue, insulin resistance, and hepatic steatosis in obesity. J Clin Invest 2006;116(6):1494–505.
[6] Suganami T, Ogawa Y. Adipose tissue macrophages: their role in adipose tissue remodeling. J Leukoc Biol 2010;88(1):33–9.
[7] Charriere G, Cousin B, Arnaud E, et al. Preadipocyte conversion to macrophage. Evidence Plasticity J Biol Chem 2003;278(11):9850–5.
[8] Tchkonia T, Morbeck DE, Von Zglinicki T, et al. Fat tissue, aging, and cellular senescence. Aging Cell 2010;9(5):667–84.
[9] O'Hara A, Lim FL, Mazzatti DJ, Trayhurn P. Stimulation of inflammatory gene expression in human preadipocytes by macrophage-conditioned medium: upregulation of IL-6 production by macrophage-derived IL-1beta. Mol Cell Endocrinol 2012;349(2):239–47.
[10] Dordevic AL, Konstantopoulos N, Cameron-Smith D. 3T3-L1 preadipocytes exhibit heightened monocyte-chemoattractant protein-1 response to acute fatty acid exposure. PLoS One 2014;9(6):e99382.
[11] Fain JN, Madan AK, Hiler ML, Cheema P, Bahouth SW. Comparison of the release of adipokines by adipose tissue, adipose tissue matrix, and adipocytes from visceral and subcutaneous abdominal adipose tissues of obese humans. Endocrinology 2004;145(5):2273–82.
[12] Hames KC, Vella A, Kemp BJ, Jensen MD. Free fatty acid uptake in humans with CD36 deficiency. Diabetes 2014;63(11):3606–14.
[13] Cai L, Wang Z, Ji A, Meyer JM, van der Westhuyzen DR. Scavenger receptor CD36 expression contributes to adipose tissue inflammation and cell death in diet-induced obesity. PLoS One 2012;7(5):e36785.
[14] Kennedy DJ, Kuchibhotla S, Westfall KM, Silverstein RL, Morton RE, Febbraio M. A CD36-dependent pathway enhances macrophage and adipose tissue inflammation and impairs insulin signalling. Cardiovasc Res 2011;89(3):604–13.
[15] Sheedy FJ, Grebe A, Rayner KJ, et al. CD36 coordinates NLRP3 inflammasome activation by facilitating intracellular nucleation of soluble ligands into particulate ligands in sterile inflammation. Nat Immunol 2013;14(8):812–20.
[16] Stewart CR, Stuart LM, Wilkinson K, et al. CD36 ligands promote sterile inflammation through assembly of a Toll-like receptor 4 and 6 heterodimer. Nat Immunol 2010;11(2):155–61.
[17] Christiaens V, Van Hul M, Lijnen HR, Scroyen I. CD36 promotes adipocyte differentiation and adipogenesis. Biochim Biophys Acta 2012;1820(7):949–56.
[18] Meex SJ, van der Kallen CJ, van Greevenbroek MM, et al. Up-regulation of CD36/FAT in preadipocytes in familial combined hyperlipidemia. FASEB J 2005;19(14):2063–5.
[19] Weber K, Schilling JD. Lysosomes integrate metabolic-inflammatory cross-talk in primary macrophage inflammasome activation. J Biol Chem 2014;289(13):9158–71.
[20] Mizunoe Y, Sudo Y, Okita N, et al. Involvement of lysosomal dysfunction in autophagosome accumulation and early pathologies in adipose tissue of obese mice. Autophagy 2017;13(4):642–53.
[21] Morgan AJ, Platt FM, Lloyd-Evans E, Galione A. Molecular mechanisms of endolysosomal Ca2+ signalling in health and disease. Biochem J 2011;439(3):349–74.
[22] Cao Q, Zhong XZ, Zou Y, Zhang Z, Toro L, Dong XP. BK Channels Alleviate Lysosomal Storage Diseases by Providing Positive Feedback Regulation of Lysosomal Ca2+ Release. Dev Cell 2015;33(4):427–41.
[23] Atakpa P, Thillaiappan NB, Mataragka S, Prole DL, Taylor CW. IP3 Receptors Preferentially Associate with ER-Lysosome Contact Sites and Selectively Deliver Ca(2+) to Lysosomes. Cell Rep 2018;25(11):3180–93 e7.
[24] Cui J, Matkovich SJ, deSouza N, Li S, Rosemblit N, Marks AR. Regulation of the type 1 inositol 1,4,5-trisphosphate receptor by phosphorylation at tyrosine 353. J Biol Chem 2004;279(16):16311–6.
[25] Harr MW, McColl KS, Zhong F, Molitoris JK, Distelhorst CW. Glucocorticoids downregulate Fyn and inhibit IP(3)-mediated calcium signaling to promote autophagy in T lymphocytes. Autophagy 2010;6(7):912–21.
[26] Zhao L, Zhang C, Luo X, et al. CD36 palmitoylation disrupts free fatty acid metabolism and promotes tissue inflammation in non-alcoholic steatohepatitis. J. Hepatol. 2018;69(3):705–17.
[27] Hudak CS, Gulyaeva O, Wang Y, et al. Pref-1 marks very early mesenchymal precursors required for adipose tissue development and expansion. Cell Rep 2014;8(3):678–87.
[28] Tang W, Zeve D, Suh JM, et al. White fat progenitor cells reside in the adipose vasculature. Science 2008;322(5901):583–6.
[29] Bora P, Majumdar AS. Adipose tissue-derived stromal vascular fraction in regenerative medicine: a brief review on biology and translation. Stem Cell Res Ther 2017;8(1):145.
[30] Lee MR, Yang HJ, Park KI, Ma JY. Lycopus lucidus Turcz. ex Benth. Attenuates free fatty acid-induced steatosis in HepG2 cells and non-alcoholic fatty liver disease in high-fat diet-induced obese mice. Phytomedicine 2019;55:14–22.
[31] Cao D, Luo J, Zang W, et al. Gamma-Linolenic Acid Suppresses NF-kappaBeta Signaling via CD36 in the Lipopolysaccharide-Induced Inflammatory Response in Primary Goat Mammary Gland Epithelial Cells. Inflammation 2016;39(3):1225–37.
[32] Cao Q, Yang Y, Zhong XZ, Dong XP. The lysosomal Ca(2+) release channel TRPML1 regulates lysosome size by activating calmodulin. J Biol Chem 2017;292(20):8424–35.
[33] Morgan AJ, Davis LC, Wagner SK, et al. Bidirectional Ca(2)(+) signaling occurs between the endoplasmic reticulum and acidic organelles. J Cell Biol 2013;200(6):789–805.
[34] Stolarczyk E. Adipose tissue inflammation in obesity: a metabolic or immune response? Curr Opin Pharmacol 2017;37:35–40.
[35] Febbraio M, Hajjar DP, Silverstein RL. CD36: a class B scavenger receptor involved in angiogenesis, atherosclerosis, inflammation, and lipid metabolism. J Clin Invest 2001;108(6):785–91.
[36] Nicholls HT, Kowalski G, Kennedy DJ, et al. Hematopoietic cell-restricted deletion of CD36 reduces high-fat diet-induced macrophage infiltration and improves insulin signaling in adipose tissue. Diabetes 2011;60(4):1100–10.
[37] Couturier J, Nuotio-Antar AM, Agarwal N, et al. Lymphocytes upregulate CD36 in adipose tissue and liver. Adipocyte 2019;8(1):154–63.
[38] Wang C, Yan Y, Hu L, et al. Rapamycin-mediated CD36 translational suppression contributes to alleviation of hepatic steatosis. Biochem Biophys Res Commun 2014;447(1):57–63.
[39] Kaur J, Debnath J. Autophagy at the crossroads of catabolism and anabolism. Nat Rev Mol Cell Biol 2015;16(8):461–72.
[40] Gao H, Li D, Yang P, et al. Suppression of CD36 attenuates adipogenesis with a reduction of P2X7 expression in 3T3-L1 cells. Biochem Biophys Res Commun 2017;491(1):204–8.
[41] Yu F, Chen Z, Wang B, et al. The role of lysosome in cell death regulation. Tumour Biol 2016;37(2):1427–36.
[42] Brady OA, Martina JA, Puertollano R. Emerging roles for TFEB in the immune response and inflammation. Autophagy 2018;14(2):181–9.
[43] Okada M, Matsuzawa A, Yoshimura A, Ichijo H. The lysosome rupture-activated TAK1-JNK pathway regulates NLRP3 inflammasome activation. J Biol Chem 2014;289(47):32926–36.
[44] Kinnunen K, Piippo N, Loukovaara S, Hytti M, Kaarniranta K, Kauppinen A. Lysosomal destabilization activates the NLRP3 inflammasome in human umbilical vein endothelial cells (HUVECs). J Cell Commun Signal 2017;11(3):275–9.
[45] Lopez Sanjurjo CI, Tovey SC, Taylor CW. Rapid recycling of Ca2+ between IP3-sensitive stores and lysosomes. PLoS One 2014;9(10):e111275.
[46] Garrity AG, Wang W, Collier CM, Levey SA, Gao Q, Xu H. The endoplasmic reticulum, not the pH gradient, drives calcium refilling of lysosomes. Elife 2016;5 pii: e15887.